Electrostatic interactions regulate the physical properties of gelatin-cellulose nanocrystals nanocomposite films intended for biodegradable packaging

Liliane S.F. Leite, Francys K.V. Moreira, Luiz H.C. Mattoso, Julien Bras

Electrostatic interactions regulate the physical properties of gelatin-cellulose nanocrystals nanocomposite films intended for biodegradable packaging

Liliane S. F. Leite[a,b,d], Francys K. V. Moreira[c], Luiz H. C. Mattoso[a,b], Julien Bras[d,e*]

[a]*Federal University of São Carlos, Graduate Program in Materials Science and Engineering (PPGCEM), 13565-905, São Carlos-Brazil, lilianesamara@gmail.com*
[b]*National Nanotechnology Laboratory for Agribusiness, Embrapa Instrumentação, XV de Novembro street, 1452, 13560–979, São Carlos-Brazil, luiz.mattoso@embrapa.br*
[c]*Department of Materials Engineering, Federal University of São Carlos, Rod. Washington Luis, km 235, São Carlos (SP), 13565–905, Brazil. francys@ufscar.br*
[d]*University Grenoble Alpes, CNRS, Grenoble INP, LGP2, F-38400 Grenoble, France,*
[e]*Nestle Research Center, 1000 Lausanne, Switzerland*

*Corresponding author: lilianesamara@gmail.com

Abstract

Cellulose nanocrystals (CNCs)-reinforced gelatin (Gel) films are appealing candidates for biodegradable packaging. However, tailoring the physical properties of Gel/CNCs films by control of pH and film-forming drying temperature continues unstudied. Here, we described the influence of pH on the physical properties of Gel/CNCs films covering different CNCs contents. The interactions between CNCs and Gel were studied by assessing the ζ-potential of Gel/CNCs suspensions under acidic (pH 3), Gel isoelectric point (pI, pH 6) and alkaline (pH 8) conditions. pH 3 promotes the electrostatic attraction, while pH 8 favors the electrostatic repulsion in the Gel-CNCs pair, increasing the suspension viscosity in both cases. The addition of 0.5 wt% CNCs decreased the water vapor permeability (WVP) of the Gel/CNCs films by 68% under electrostatic attractive forces and by 39% at the gelatin pI. The addition of 5 wt% CNCs at pH 3 resulted in the formation of complex coacervates, which decreased the mechanical properties and increased the WVP of Gel/CNCs films. Increasing pH above the Gel pI remarkedly increased the gelatin renaturation as triple helices, which was found to be key for increasing by 152% and 56% the Young's modulus and tensile strength, respectively, of the Gel/CNCs films with 0.5 wt% CNCsFilm-forming drying temperatures had an inverse effect on the triple helix content, and, consequently, on the physical properties of the Gel/CNCs films. These findings denote that modulating pH, CNCs amount, and drying temperature is a suitable strategy for tailoring the properties

of nanocellulose-reinforced gelatin films for an extended range of food packaging applications.

Keywords: Gelatin, cellulose nanocrystal, electrostatic interaction, mechanical properties.

1. Introduction

The growing plastic production has led to a global waste disposal crisis. Nowadays, researches are focused on solving this problem by obtaining biodegradable packaging. Biopolymers, including proteins and polysaccharides, are the main natural resources employed to develop biodegradable films (Esteghlal, Niakousari, & Hosseini, 2018). Proteins are natural polyelectrolytes that have attracted great interest due to their unique properties (Al-Tayyar, Youssef, & Al-hindi, 2020; Moustafa, Youssef, Darwish, & Abou-Kandil, 2019), in particular, their ability to form self-assembled structures, such as ionic complexes obtained by the interactions with polysaccharides carrying opposite charges(Derkach, Kuchina, Kolotova, & Voron'ko, 2020). These structures are promising for the creation of new materials applicable in pharmacy, medicine (Vuillemin, Michaux, Muniglia, Linder, & Jasniewski, 2019; Zhao, Skwarczynski, & Toth, 2019), and food packaging (da Silva, de Oliveira, Simas, & Riegel-Vidotti, 2020; Hosseini, Rezaei, Zandi, & Farahmandghavi, 2015).

Gelatin is a protein obtained by the partial hydrolysis of collagen at controlled temperature and pH conditions (Joshi, Rawat, & Bohidar, 2018). This protein is cheap, commercially available, biodegradable, in addition to presenting good processability and film-forming properties (Wang et al. 2014). The mechanical behavior of gelatin gels and films is related to the regeneration of gelatin as crystalline triple helixes. Gioffrè et al. (2012) investigated the pH effect on the mechanical properties of pigskin type A gelatin films and observed that pH values higher than 9 and lower than 5 considerably reduced the triple helix content and, consequently, the mechanical properties of the films.

Gelatin films are moisture-sensitive and exhibit low water vapor barrier and mechanical resistance under high relative humidity due to the hydrophilicity of the polypeptide chains (Gómez-Guillén et al. 2009). A suitable approach to overcoming these limitations of gelatin films is the use of cellulose nanocrystals (CNCs) as nano-sized fillers (Hosseini & Gómez-Guillén, 2018),. CNCs are one of the most studied

polysaccharide-based nanomaterials in polymer nanocomposites (Espino-Pérez, Domenek, Belgacem, Sillard, & Bras, 2014; Noorbakhsh-Soltani, Zerafat, & Sabbaghi, 2018). CNCs are suitable for such purposes due to their large elastic modulus (~143 GPa) biodegradability and abundance (Dufresne, 2018) (Habibi, Lucia, & Rojas, 2010).

Several reports have described a joint synergistic effect between gelatin and CNCs toward the formation of percolated networks stabilized by hydrogen bonding. George & Siddaramaiah (2012) showed that the use of CNCs, obtained from bacterial cellulose, at a weight fraction of 4%, maximized the tensile strength, tensile modulus, and stiffness of gelatin films. Santos et al. (2014) demonstrated that tilapia gelatin films had a high stiffness and good ductility up to a CNCs loading of 5 wt%. Above this concentration, the mechanical properties tended to reach a plateau. Mondragon et al. (2015) showed that cellulose nanofibers (CNFs) and CNCs improved the oxygen gas barrier properties of gelatin films and that these nanocelluloses did not significantly improve the tensile properties of the films when used at weight fractions ≤ 10%. More recently, Leite et al. (2020) demonstrated that adding 0.5 wt% CNCs increased the tensile strength and Young's modulus of gelatin films obtained by continuous casting by 77 % and 48 %, respectively.

To the best of our knowledge, no research has been published on the reinforcing effect of CNCs on gelatin films under different types of electrostatic interactions. The knowledge of these intermolecular interactions is crucial for understanding the structure of Gel/CNCs films, as well as for the development of packaging films with tunable physical properties. Furthermore, there is no report that examines the structure and mechanical properties of Gel/CNCs films as influenced by the casting temperature. This work aimed to investigate the effect of CNCs, pH, and drying temperature on the triple helix content, mechanical, thermal, and barrier properties of gelatin films obtained by bench casting.

2. Materials and methods

2.1. Materials

Bovine gelatin (Bloom Strength-190) was kindly supplied by Gelco Gelatinas do Brazil Ltda (Pedreira, SP). CNCs isolated from wood pulp by sulfuric acid hydrolysis and with crystallinity index of 82% (Fig. S1) and delivered as a dried powder were purchased from Celluforce Inc. (Windsor, Québec, Canada).Glycerol and ethanol were

purchased from Across Organics (USA). All chemicals were analytical grade and were used as purchased.

2.2. Methods

2.2.1. Preparation of nanocomposite films

The nanocomposite films were prepared by solvent casting. The gelatin (Gel)powder was hydrated in distilled water (10 g/100 g) at 24 °C for 5 min and heated at 60 °C under stirring for 15 min. The Gel solution pH was adjusted to 3, 6, and 8 with 3M HCl or NaOH. Glycerol (2 g/100 g of protein) was added to the Gel solution under stirring for 5 min. The obtained Gel/glycerol solution was mixed with the CNCs suspension at desired contents (0 wt%, 0.5 wt%, and 5.0 wt%, on a dry gelatin mass basis) and stirred for additional 5 min. The final film-forming solutions (FFS) (45 mL) were cast on glass plates (40 cm× 25 cm), covered with a polyester film (Mylar®, DuPont, Brazil) to facilitate film peeling off after drying in an oven at 25, 35 and 80 °C for 24 h. Film samples were conditioned at 50% relative humidity (RH) in a ventilated climatic chamber and 25 °C for at least 24 h prior to any testing.

2.3. Characterizations

2.3.1. Determination of Zeta potentials (ζ-potentials)

ζ-potentials of aqueous CNCs dispersion, pure Gel solution and Gel/CNCs FFS obtained at pH 3, 6 and 8 (0.5 wt% and 5.0 wt% CNCs on a dry gelatin mass basis) diluted to 0.25 wt% were analyzed at 25 °C using a Zetasizer Nano-ZS (Malvern Instruments Inc., UK). Each sample was mixed with a sonicator (Branson 450 Sonifier, USA) for 5 min with a microtip before analysis. The measurements were performed in triplicate.

2.3.2. Rheological study

The apparent viscosity and flow behavior of the FFS (pure Gel and Gel/CNCs with 0.5 and 5 wt% CNCs at pH 3, 6 and 8) were evaluated on a Physica MCR101

rheometer (Anton Paar, Austria) using the concentric cylinder geometry at 40 °C. The shear rate was varied from 0 to 150 s^{-1} in 10 min. Oscillatory shear deformation tests were also carried out to determine the storage modulus (G') and loss modulus (G") of the FFS at a constant strain of 1% and frequency of 1 Hz in the temperature range of 60-20 °C using heating/cooling rate of 0.02 °C s^{-1}. Strain values were chosen to be within the linear viscoelastic region based on preliminary measurements. The flow behavior was described by fitting the experimental data to the Power Law model (Eq. 1).

$$\sigma = k\dot{\gamma}^{n} \quad (1)$$

where σ is the shear stress (Pa), $\dot{\gamma}$ is the shear rate (s^{-1}), k is the consistency coefficient (Pa s^n) and n is the flow behavior index.

2.3.3. Polarized light optical microscopy

Optical images of Gel/CNCs films were taken between crossed polarizers to evaluate the dispersion of the CNCs within the gelatin matrix. The samples were imaged by polarized optical microscopy taken at 10-fold magnification using a microscope Zeiss Axio Vert.A1 (Carl Zeiss Microscopy).

2.3.4. Scanning electron microscopy (SEM)

Film surface and the cross-sectional surface were investigated using a JEOL Scanning Electron Microscope (SEM, model Quanta200, FEI, the Netherlands). The samples were first cryo-fractured in liquid N_2 and then fixed onto 90° specimen mounts to be coated with a ca. 5-nm-thick gold layer in an argon atmosphere. The SEM images were taken at accelerating voltages below 10 kV using the secondary electron mode.

2.3.5. X-ray diffraction (XRD) analysis

X-ray diffraction patterns were acquired from 2 ° to 60 ° (2θ) using a Panalytical diffractometer (X'Pert Pro MPD-Ray) with Ni-filtered Cu Kα radiation (λ = 1.54 Å) generated at a voltage of 45 kV and current of 40 mA. The amount of triple helix

configuration (X_c in %) in the Gel/CNCs films was calculated in duplicate for each sample using Eq. 2.

$$Xc = [A_c/(A_{c+} A_a)]\, x100 \quad (2)$$

where Ac is the area of the diffraction peak at ~2θ = 8°, corresponding to the triple helix configuration of gelatin chains, and Aa is the area under the hump located at ~2θ = 21°, corresponding to the fraction of amorphous domains in the gelatin films. (Díaz-Calderón, Flores, Gonz, & Enrione, 2017).

2.3.7. Tensile tests

The tensile properties of the films were determined by the ASTM D882-09 standard method (2009). The film specimens (17 cm x 1 cm) were prepared and equilibrated in a ventilated climatic chamber at 23 ± 1 °C and 50 ± 5% RH for 48 h. The tests were carried out in an Instron Universal Testing Machine (model 5569, Instron Corp., USA) equipped with a 100 N load cell. The specimens were stretched using crosshead speed of 10 mm/min with clamps initially separated by 100 mm. Tensile strength, Young's modulus, and elongation at break were calculated from the stress-strain curves. Thicknesses were measured using a digital micrometer (Adamel Lhomargy) to the nearest 0.001 mm with ten random measurements per film. The tensile tests were performed with five replicates per film sample.

2.3.8. Water vapor permeability (WVP)

WVP was determined using the ASTM E-96-01. The preconditioned film was sealed onto the opening of an aluminum permeation cup (28 mm internal diameter) containing dried calcium chloride. The cup was kept in a ventilated climatic chamber at 23 ± 1 °C and 50 ± 5% RH. The cup was weighed at least four times for at least 7 days under this controlled environment. For each film, three replicates were performed. The WVP g mm m^{-2} h^{-1} kPa^{-1} was determined using Eq. 3:

$$WVP = (\Delta m/\Delta t)\, x\, (L/A\Delta P) \quad (3)$$

where Δm/Δt is the mass gain over time (g h^{-1}), A is the exposed film area (m^2), L is the film thickness (mm), and ΔP is the difference of partial pressure.

2.3.9. Water solubility (WS) determination

The gelatin films were cut into rectangular (1 cm × 1 cm) specimen and pre-dried at 105 °C for 24 h. The dried specimens were accurately weighed (initial dry weight, w_0), placed in distilled water (30 mL), and stirred at 25 ± 1 °C for 24 h. Filter paper number 1 was prepared by drying at 105 °C for 24 h. Then, the film was poured onto the filter paper and dried at 105 °C for 24 h and weighed (final dry weight, w_1). WS was measured in triplicate following calculated using Eq 4.

$$WS\ (\%) = [(w_0 - w_1)/w_0] \times 100 \quad (4)$$

2.3.10. Thermogravimetric analysis (TGA)

Thermogravimetric analysis was carried out in a Q500 equipment (TA Instruments, USA). About 10 mg of each film sample was taken in a standard Ptcrucible and heated from 25 °C to 600 °C with heating rate of 10 °C min^{-1}, under inert atmosphere of nitrogen (60 mL/min). Samples before the TGA tests were conditioned in a ventilated climatic chamber at 23 ± 1 °C and 50 ± 5% RH for 48 h.

2.3.11. Statistical analysis

Data were subject to analysis of variance (ANOVA). The mean values were compared using the Tukey's test at a confidence level of 95 % ($p<0.05$) using the Origin software (OriginLab, Northampton, USA).

2. Results and discussion

3.1 Physical and rheological properties of Gel/CNCs film-forming solutions

ζ-potentials provide evidence of the net charges on particle surfaces as a function of pH. Fig. 1 illustrates the evolution of the ζ-potential of gelatin solution and CNCs suspension upon pH variation. The isoelectric point (pI) of gelatin solution occurred at around pH 6, at which a null ζ-potential was observed. This is in agreement with previously reported data for type B gelatins (pH 4.5-6.0) (Ahmed, 2017). Gelatin has the ability to present different charges depending on the pH (Gioffrè et al. 2012). At pH < pI, the gelatin solution showed a net positive charge, which was attributed to the protonation of the amino groups ($-NH_3^+$), while at pH > pI the solution showed a net negative charge, due to ionization of the carboxyl groups ($-COO^-$). For the CNCs suspension, the ζ-potential value was found to be negative regardless of the pH. The ζ-potential value of CNCs suspension was around -50 mV indicating a stable suspension in water. According to Lin, Gu, & Cui (2019), ζ-potentials (< -30mV and > + 30 mV) could maintain a stable colloidal system due to the repelling forces between particles. This value can be attributed to the sulfate groups (SO_3^-) grafted on the CNCs surface (Habibi et al. 2010), agreeing with a previous study (Silva et al. 2019).

In aqueous solutions, electrostatic charges are one of the main driving forces for interactions between charged biopolymers (Behrouzain, Razavi, & Joyner, 2020). For the Gel/CNCs FFS at pH < pI, the gelatin and CNCs are expected to form complexes stabilized by electrostatic attractive interactions, while at pH > pI the mixture should exhibit electrostatic repulsive interactions between the negatively charged COO^- groups of gelatin and SO_3^- groups of CNCs. Similar behaviors for protein-polysaccharides were recently reported elsewhere (Razzak, Kim, & Chung, 2016; Voron'ko, Derkach, Kuchina, & Sokolan, 2016). As expected, the ζ-potential of the Gel/CNCs FFS at pH 6 and pH 8 decreased with increasing the CNCs concentration (Fig. S2). However, at pH 3, the addition of CNCs did not change significantly the ζ-potential values of the Gel/CNCs FFS compared to the pure Gel solution at the same pH, confirming that electrostatic attractive interactions occurred between the positively charged gelatin chains and negatively charged CNCs in acidic medium.

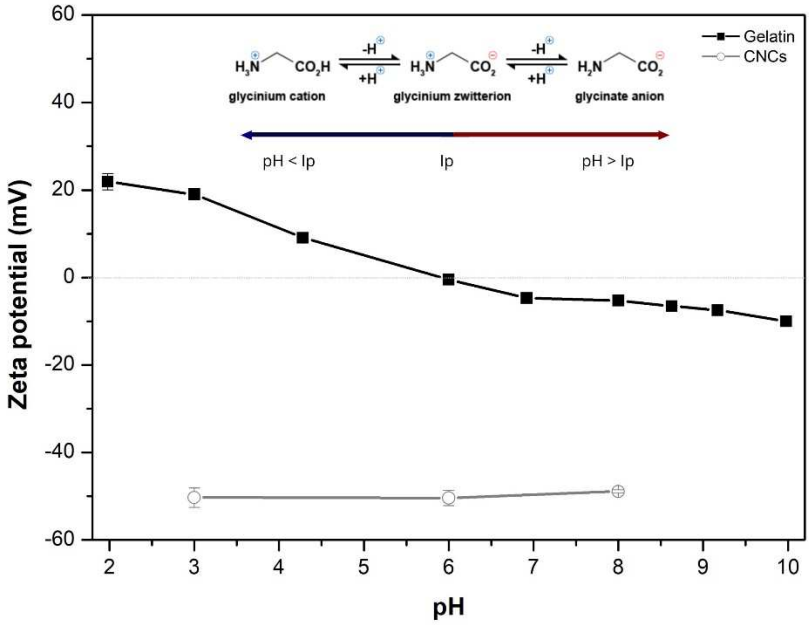

Fig.1. ζ-Potential values of neat Gel solution and CNCs suspension (0.25 wt%) at 25 °C as a function of pH.

The rheological behavior of the Gel/CNCs FFS was evaluated at different pH. The apparent viscosity and parameters calculated by Ostwald de Waele model are presented in Table 1. The flow curves are shown in Fig. S3. Experimental shear stress *vs*. shear rate curves were fitted to the Ostwald de Waele model ($r^2 > 0.99$), which has been widely used to describe non-Newtonian fluids over the most important shear rate ranges (Ahmed, 2017). All the FFS exhibited a shear-thinning behavior ($k > 0$; $0 < n < 1$) and their apparent viscosities (η_{ap}) decreased as the shear rate increased. This pseudoplastic behavior of Gel/CNCs FFS became progressively more pronounced at high CNCs contents and with attractive (pH 3) and repulsive (pH 8) electrostatic conditions. As expected, the addition of CNCsincreased the apparent viscosity of the Gel/CNCs FFS. The electrostatic attraction between the CNCs and gelatin molecules at pH 3 leads to the formation of gel networks through ionic cross-linking (Kwak, Lee, Park, Lee, & Jin, 2020). By contrast, the electrostatic repulsive forces between gelatin and CNCs at pH 8 can stretch the gelatin molecules and favor mutual orientation of macromolecules and creation of non-covalent interactions (Voron'ko et al. 2016). This could decrease the mobility of protein molecules, thus increasing the resistance between gelatin FFS layers. The minimum viscosity was found at the Gel isoelectric point (pH 6),

Table 1. Apparent viscosity (η_{ap}) parameters of Ostwald de Waele model (consistency index (K), and flow index (n)) and transition temperatures of Gel/CNCs film-forming solution at pH 3, 6, and 8.

	Gel/CNCs film-forming solution								
	Electrostatic attractive forces pH 3			**Isoelectric point pH 6**			**Electrostatic repulsive forces pH 8**		
CNCs (wt%)	0	0.5	5.0	0	0.5	5.0	0	0.5	5.0
	Parameters of Ostwald de Waele model								
k (mPa s^n)	0.01	0.03	1.03	0.01	0.03	0.01	0.01	0.02	2.25
n	0.92	0.83	0.32	0.97	0.97	0.90	0.90	0.96	0.24
r^2	0.993	0.998	0.997	0.999	0.999	0.992	0.999	0.999	0.990
η_{ap} (mPa) at 1 s^{-1}	10.1	25.0	887.3	10.9	17.5	12.7	7.79	14.0	1788
	Transition temperature (°C)								
Gel-sol	32.1	32.0	Nd	34.6	35.1	35.0	35.6	35.1	37.8
Sol-gel	19.4	22.7	Nd	22.7	22.8	22.6	22.4	22.6	Nd

Nd: not detected.

Dynamic rheological measurements can be used to monitor structures in weak gels or viscoelastic fluids (Behrouzain & Razavi, 2018). These measurements provide key information for gel processability in continuous solvent casting or 3D printing. Fig. 2 shows the storage modulus (G') and loss modulus (G") of the Gel/CNCs FFS with 0 and 5 wt% CNCs at different pH obtained from heating and cooling scans. All the samples presented a similar rheological behavior, regardless of the pH or CNCs content. The viscoelastic modulus (G'or G") were higher at lower temperatures (gel-like domain) than at higher temperatures (sol-like domain), with a well visible inflection between both domains (G'=G"). This inflection is typical of physical gels, and is defined as the gel-sol transition (Fig. 2a,c) and sol-gel transition (Fig. 2b,d) on the heating and cooling curves, respectively. Similar profiles have been observed in gelatin-based systems by several authors (Alexandre, Lourenço, Bittante, Moraes, & Sobral, 2016; Fernando et al. 2014). The gel-sol temperatures (heating curves) of the Gel/CNCs

FFS was more affected by the Gel/CNCs electrostatic interactions (Table 1). A remarkable hysteresis, of about 12 °C, was also noticeable (Fig. S3). Furthermore, the addition of 5.0 wt% CNCs to the gelatin solution at pH 3 resulted in an elastic gel-like behavior (G' > G") even above the gel-sol temperature. According to Qiao et al. (2016), proteins can form complex coacervates through interactions of oppositely charged particles, as previously indicated by the ζ-potential values of the Gel/CNCs FFS at pH 3. Complex coacervation can lead to precipitation of polymer complexes through the formation of a dense media that can be treated as being composed of interconnected gel-like network structures, consistent with the assumption that the CNCs are electrostatically "cross-linked" along the gelatin chains. Consequently, the gel-sol and sol-gel transitions of the Gel/CNCs FFS were not observed due to Gel/CNCs electrostatic attractive forces. The Gel/CNCs FFS with 5% CNCs at pH 8 also did not exhibit the sol-gel transition and presented a solid-like behavior, indicating the existence of physical crosslinks by hydrogen bonding as mentioned before.

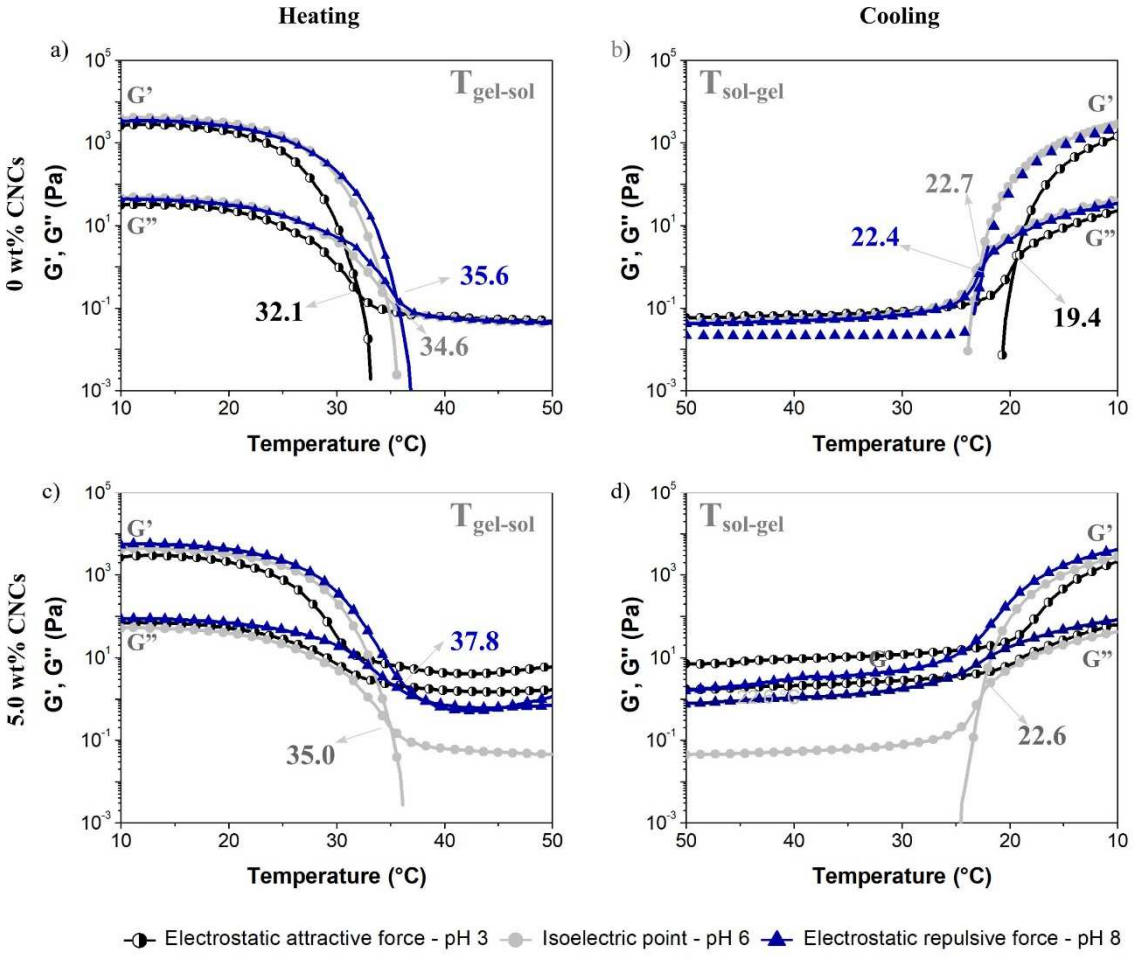

Fig. 2 Viscoelastic modulus of Gel/CNCs FFS at different pH and CNCs contents. Heating (a and c) and cooling (b and d) at 1 °C min^{-1}.

3.2. Characterization of Gel/CNCs nanocomposite films

3.2.1 Morphological and structural characterizations

The photographs of the Gel/CNCs films are shown in Fig.3a. All the films displayed good macroscopic homogeneity and transparency. Cracks on their surface were also absent. The morphology of the Gel/CNCs films obtained from different pH was investigated by SEM (Fig.3b). The Gel film with 5.0 wt% CNCs at pH 3 showed aggregates (white arrows), on both cross-sectional and air-drying surfaces, suggesting the formation of large CNCs-gelatin coacervates. This was also confirmed by polarized light optical microscopy images (Fig. S4). The same effect was observed by Li et al. (2018) for gelatin/gum arabic mixtures at pH 3.5. They found that complex coacervates were spontaneously formed between gelatin and gum arabic by effective electrostatic interactions at low pH, where gelatin and gum arabic presented opposite surface charges. By contrast, the electrostatic attraction between gelatin and CNCs is weakened by increasing the pH, and the coacervates disappeared at pH 6 and 8 (Fig. 3b). The Gel/CNCs films showed homogeneous and continuous surface with no white dots, which suggest that the CNCs were homogeneously distributed throughout the film structures (Leite, Battirola, Escobar da Silva, & Gonçalves, 2016).

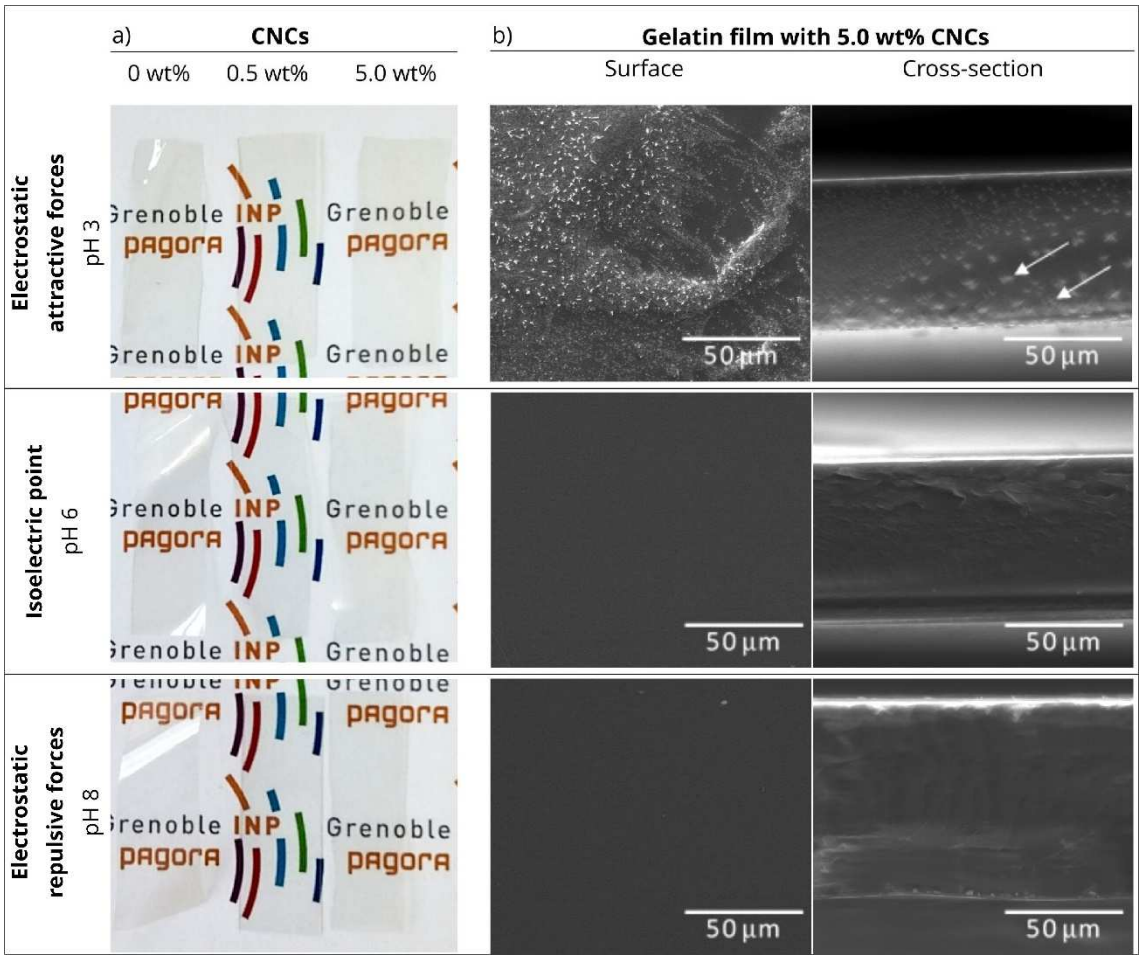

Fig.3. (a) Photographs of Gel/CNCs films with different CNCs contents, (b) SEM micrographs of air-drying and cross-sectional surfaces of Gel/CNCs films with 5.0 wt% CNCs at pH 3, pH 6 and pH 8. White arrows indicate CNCs-gelatin coacervates at pH 3.

The XRD patterns of the films obtained from different pH and CNCs contents are shown in Figs. 4a-b. The formation of gelatin film is accompanied by the renaturation of triple helical structures of protein molecules (Lin et al. 2019). The XRD diffractograms showed a wide background with a band at 2θ ~21°, which is typically related to the large amorphous Gel fraction (Bigi, Panzavolta, & Rubini, 2004). The band at 2θ ~8° has been previously attributed to the presence of triple helix structure present in collagen and renaturated gelatin (Quero et al. 2018). The area of this peak has been found to be directly related to the triple helix content of gelatin-based composites (Badii et al. 2014; Bigi et al. 2004; Yakimets et al. 2005). As seen in the insert in Figs. 4a-b, the band area at 2θ ~8° changed with the pH and CNCs content. The triple helix content was 9.4, 6.3, and 6.9% for Gel films with 0 wt% CNCs at pH 8, 6 and 3,

respectively (Table S1). According to Ahsan & Rao (2017), the triple helix content of type B gelatin decreases with decreasing pH, most likely due to the structural changes in gelatin to mild denaturation, which was complete at around pH 2.5. The highest triple helix content (13.5%) was observed in the film with 0.5 wt% CNCs at pH 8. This behavior may result from deprotonation of the gelatin molecules at alkaline pH, favoring the formation of hydrogen bonds (Ahmed, 2017), which are essential to stabilize the gelatin triple helices. The formation of hydrogen bonds between CNCs and gelatin chains (both inside and outside helical fragments), also favors the regeneration and stabilization of triple helix structures (Bigi et al. 2004; Gioffrè et al. 2012). However, the addition of 5.0 wt% CNCs markedly diminished the triple helix content, suggesting an increased random coil conformation of gelatin chains. Similar behavior was observed by Yakimets et al., (2005) who found changes in the structural and molecular order of gelatin films induced by water content. This result may also suggest that the folding process from random coil to triple helix is influenced by pH and CNCs amount.

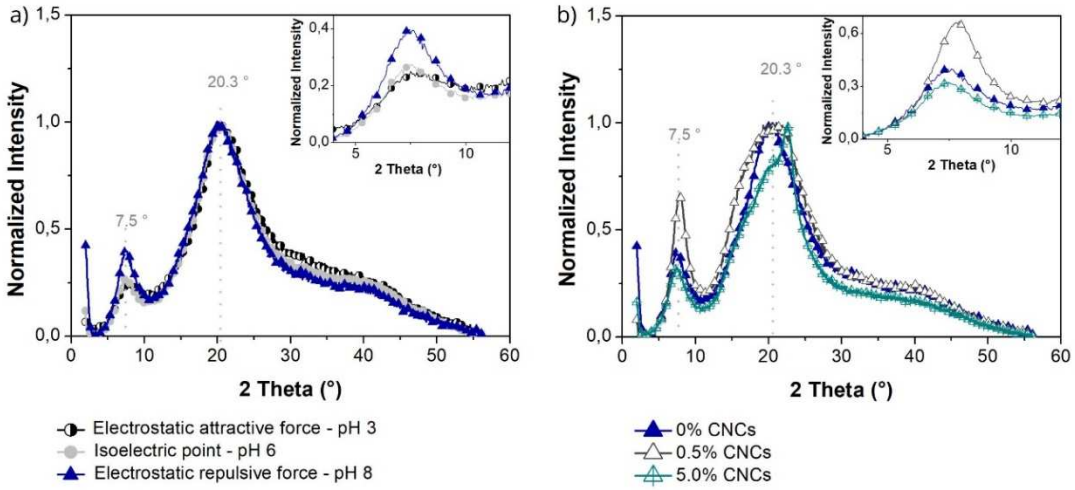

Fig.4. XRD patterns of (a) pure Gel film obtained from FFS with pH 3, 6 and 8 (b) Gel/CNCs films obtained from pH 8 and different CNCs contents. The magnified view of the 2θ range 3 – 12º is shown as an insert.

3.2.2 Mechanical properties

The Young's modulus, elongation at break, and tensile strength of Gel/CNCs films are presented in Fig.5. The nanocomposite films containing 0.5 wt% CNCs at pH

3 and 8 presented significantly increased Young's modulus and tensile strength, and decreased elongation at break compared to the pure Gel films ($p < 0.05$). This effect was more pronounced at pH 8, whose Young's modulus and tensile strength increased by 152% and 56%, respectively ($p < 0.05$). At pH 3, the increases in Young's modulus and tensile strength for the 0.5 wt% CNCs content may be attributed to the electrostatic attractive interaction between gelatin and CNCs. When pH was increased to 6, no significant changes in the tensile properties of the 0.5 wt% Gel/CNCs film were observed ($p > 0.05$), most likely due to the reduction in the electrostatic interactions above the gelatin pI. At pH 8, the increases in Young's modulus and tensile strength are most likely due to the regeneration of triple helixes, which increases the overall crystallinity of the films (Bigi et al. 2004). Gioffrè et al. (2012) observed that pH higher than 9 and lower than 5 considerably reduced the triple-helix content and, consequently, reduced the Young's modulus and elongation at break of pigskin type A gelatin films. Quero et al. (2018) attributed the improved mechanical performance of 15 wt% microfibrillated cellulose (MFC)-added salmon gelatin films to the high triple-helix content of the nanocomposites compared to similar nanocomposites obtained from bovine gelatin.

When the CNCs content was increased to 5.0 wt%, the Young's modulus and tensile strength of the Gel/CNCs films slightly increased at the Gel pI (pH 6), but drastically decreased at pH 3 and 8 ($p < 0.05$). For the acidic condition (pH 3), such decreases could be attributed to the large aggregates formed by the CNCs-gelatin complex coacervates (Celebi & Kurt, 2015). These aggregates provided a heterogeneous distribution of the CNCs within the gelatin matrix, as revealed by SEM (Fig.3b), acting as defects in the film structure, thus reducing the mechanical resistance of the Gel/CNCs nanocomposites (Cao, Zavattieri, Youngblood, Moon, & Weiss, 2016). For the alkaline condition (pH 8), despite the uniform dispersion of the CNCs within the Gel matrix, the triple-helix content decreased, and the electrostatic Gel-CNCs repulsion in the films may have increased the free volume in the gelatin matrix (Lin et al. 2019). These behaviors could explain the reductions in Young's modulus and tensile strength, and the significant increase in elongation at break, respectively, for the 5 wt% CNCs-added Gel nanocomposite film ($p < 0.05$) at pH 8. The moderate but gradual increases in Young's modulus and tensile strength at pH 6 may relate to the lower triple helix content compared to pH 8. These lowered effects also led the Gel/CNCs nanocomposites obtained from the Gel pI to show a more ductile mechanical behavior, as illustrated in

Fig. 5d. Overall, these results denote that pH and CNCs content significantly regulate the mechanical properties of gelatin films.

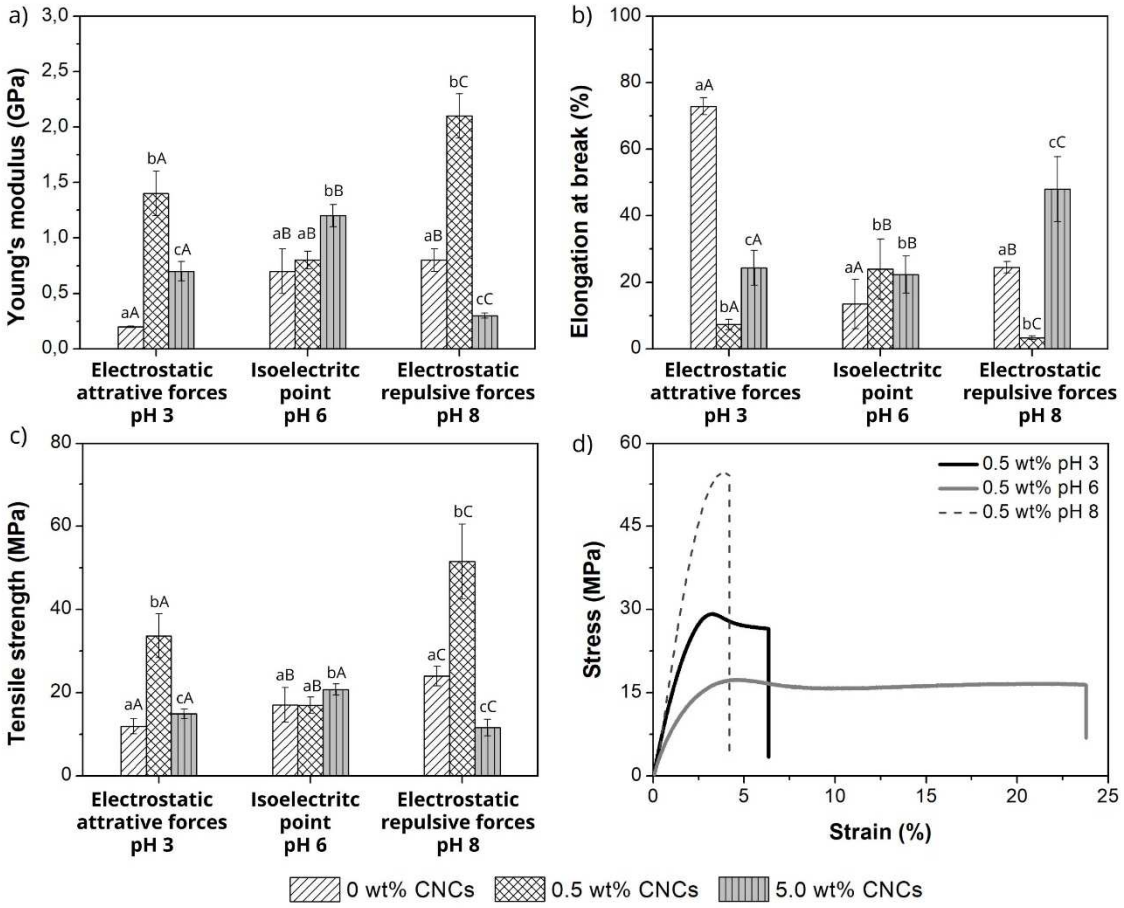

Fig. 5. (a) Young's modulus, (b) elongation at break, (c) tensile strength, and (d) stress-strain curves of Gel/CNCs films as a function of pH and CNCs content. Lowercase letters (a, b, c) - Mean values in the same pH bearing the same letter are not statistically different according to the Tukey's test ($p > 0.05$). Capital letters (A, B, C) - Mean values in the same CNCs amount bearing the same letter are not statistically different according to the Tukey's test ($p > 0.05$).

3.2.3 Water affinity and barrier properties

The WVP of the Gel/CNCs films obtained from different pH and CNCs contents are presented in Table 2. No significant differences ($p > 0.05$) among the WVP for gelatin films with 0% CNCs were observed concerning the pH variations. These results agree with previous findings on fish myofibrillar protein films (Shiku et al. 2003), but

differ from those previously reported for soy protein isolate films, which showed lower WVP at pH values above the soy protein isoelectric point (Gennadios, Brandenburg, Weller, & Testin, 1993). The WVP at 50% RH of the Gel/CNCs films were lower than those observed for other films based on gelatin at 0% RH (B.-S. Chiou et al. 2008); the results found were close to 1.8 g mm/m^2 h kPa (25 °C at 0% RH) for bovine and porcine gelatin films. The addition of CNCs to gelatin at pH 3 and pH 6 significantly decreased the WVP by 68% and 39% ($p < 0.05$), respectively, of the resulting films. According to Qiao et al. (2013), the addition of counterions screens the electrostatic repulsions between charges in the polymer, which, in turn, allows the chains to collapse and assume a more compact conformation. In a previous study, Santos et al. (2014) reported that the WVP of protein films decreased by increasing the CNCs loading. They found that fish gelatin films with 15 wt% CNCs exhibit WVP values of approximately 2 g mm/m^2 h kPa (25 °C at 85% RH). George & Siddaramaiah (2012) reported that 4 wt% of bacterial cellulose nanocrystals reduced the WVP of gelatin and attributed this to the low hygroscopicity of the highly crystalline cellulose nanocrystals (Fig S3). They found WVP values around 0.175 g mm/m^2 h kPa (25 °C at 50% RH). By contrast, as expected, the addition of CNCs to the gelatin matrix at pH 8 increased the WVP since the electrostatic repulsion in alkaline Gel/CNCs films can increase the free volume, which resulted in greater water vapor diffusion. Overall, the WVP values of the gelatin/CNCs films in the present study were lower than those of previous gelatin films reinforced with CNCs.

The water solubility results are summarized in Table 2. No film fully dissolved or broke apart after 24 h at 25 °C, suggesting that they were formed by stable network. The solubility of the Gel films decreased by increasing the pH since higher pH favors the increase of protein-protein interactions and the exposition of hydrophobic groups that increase surface hydrophobicity gelatin and decrease the water solubility (Díaz, Candia, & Cobos, 2017) The addition of CNCs at pH 6 and pH 8 did not significantly ($p < 0.05$) change the Gel film solubility. However, a drastic decrease in water solubility was observed at 0.5 wt% CNCs and pH 3. This improvement in the water resistance can be attributed to the formation of the Gel-CNCs complex coacervates, as shown in the polarized light optical microscopy images (Fig. S4). These results are in agreement with Esteghlal et al. (2018), who suggested that the decrease in solubility is due to charge reduction after complexation and formation of crosslinked gelatin-CMC films. Yin et al. (2005) also found a similar behavior for chitosan/gelatin polyelectrolyte complexes.

Table 2. Water vapor permeability at 50% RH and 25 °C and water solubility of the gelatin films with different pH and CNCs content.

CNCs content (%)	WVP (g mm/ m^2 h KPa) Electrostatic attractive force	Isoelectric point (pI)	Electrostatic repulsive force
	pH 3	pH 6	pH 8
0	0.204 ± 0.085^{aA}	0.180 ± 0.027^{aA}	0.131 ± 0.020^{aA}
0.5	0.065 ± 0.013^{bA}	0.111 ± 0.022^{bB}	0.158 ± 0.022^{aB}
5.0	0.189 ± 0.009^{aA}	0.109 ± 0.019^{bB}	0.262 ± 0.034^{bC}
		Water solubility (%)	
0	65.3 ± 2.55^{aA}	31.7 ± 4.81^{aB}	15.7 ± 3.30^{aC}
0.5	14.6 ± 1.24^{bA}	21.5 ± 6.55^{aA}	16.9 ± 4.97^{aA}
5.0	42.1 ± 2.52^{cA}	32.4 ± 1.30^{aB}	17.1 ± 9.46^{aB}

Mean ± standard deviation. Lowercase letters (a, b, c) - Mean values in the same column bearing the same letter are not statistically different according to the Tukey's test ($p > 0.05$). Capital letters (A, B, C) - Mean values in the same row bearing the same letter are not statistically different according to the Tukey's test ($p > 0.05$).

3.2.4 Themo stability

The Gel/CNCs films were further characterized by TGA and the degradation temperatures are reported in Table S2. All TGA curves are presented in Fig. S5. All samples followed a similar decomposition profile. The first mass loss was due to moisture and volatiles evaporation (Noorbakhsh-Soltani et al. 2018). Pure gelatin films at pH 3 showed the lowest moisture content (3%) and the addition of 5.0 wt% CNCs increased the weight loss at this stage, with exception of the Gel/CNCs film at pH 6 (Table S2), which may be due to less availability of free hydroxyl groups of the gelatin matrix due to hydrogen bonding with CNCs at pH 6. This result is in line with the increase in Young's Modulus and reduction in the WVP of the Gel/CNCs film with 5.0 wt% at pH 6. A significant mass loss occurred at temperature (T_{onset}) above 200 °C, mainly associated with the decomposition of gelatin and glycerol molecules. The thermal stability of Gel films increased near the gelatin isoelectric point, which is the result of a more compact form of gelatin (Alberto & Gabriela, 2012). This result is in agreement with Gioffrè et al. (2012), who reported a reduction in the thermal stability of

gelatin films prepared at relatively high and low pH. The higher thermal stability was found for the Gel/CNCs films with 0.5% CNCs at pH 3 and pH 8, which showed increases of 14.4 and 15.3 °C in the T_{onset}, respectively, when compared to pure gelatin films at the same pH. This improvement might be attributed to the formation of more rigid structures, like the Gel-CNCs coacervates formed at pH 3. This may also be related to the high concentration of triple helix structures present in Gel/CNCs films at pH 8, as shown by XRD (Fig.4). In addition, the formation of hydrogen bonds between CNCs and gelatin can also influence the protein denaturation process and, as a consequence, lead to an increased film thermal stability, as justified by George & Siddaramaiah, (2012). Previous studies have shown that the addition of CNCs increased 9 °C T_{onset} for gelatin films with 10 wt% CNCs (Mondragon et al. 2015), 10.6 °C for gelatin films with 2.5 wt% CNCs (Leite, Ferreira, Corrêa, Moreira, & Mattoso, 2020) and a decrease of around 6 °C for gelatin films with 1.5 wt% CNCs, when compared to pure gelatin films (Alves, dos Reis, Menezes, Pereira, & Pereira, 2015).

The gelatin film with 0.5 wt% CNCs obtained from pH 8, which had the highest triple helix content, was chosen to evaluate the effect of the drying casting temperature on the mechanical, thermal and barrier properties of Gel/CNCs nanocomposites. The obtained results for the film samples dried at 25 °C ("cold-dried"), 35 °C (gelation temperature) and 80 °C ("hot-dried") are listed in Table 3. The gelatin films dried at 25 °C showed the highest Young's modulus and tensile strength. This was likely due to the fact that cold-dried films had a longer drying time (24 h), i.e. sufficient time for the reorganization of gelatin structures as triple helices than the hot-dried films (6 h). Chiou et al. (2009) observed that gelatin films dried below their gelation temperature contained crystallinity triple-helix structures, whereas films dried above their gelation temperature were virtually amorphous. Films with helical structures exhibit higher tensile strength and Young's modulus than amorphous films (Badii, MacNaughtan, Mitchell, & Farhat, 2014).

Furthermore, the thermal stability of gelatin films increased when the drying temperature was decreased (Fig. S5). These results might be explained by the larger amount of energy needed to break the hydrogen bonds in the triple helix structures formed in the cold-dried gelatin films (Fig. S6). The WVP results showed no statistical difference concerning the drying temperature ($p > 0.05$). Bor Sen Chiou et al. (2008) showed that mammalian gelatin films had higher levels of renaturation than fish gelatin films. However, the authors observed that this greater amount of helical structures did

not lead to better water barrier properties, proving that WVP is not proportional to the renaturation level in gelatin films. The mechanical, thermal and barrier results suggest that the drying temperature used in the casting process and the addition of CNCs are significant factors that affect the structure and physical properties of Gel/CNCs films.

Table 3: Tensile, thermal properties, water vapor permeability, and triple-helix content of gelatin films with 0.5% CNCs at pH 8 as a function of different drying temperatures.

Drying temperature (°C)	Young's modulus (GPa)	Tensile strength (MPa)	Elongation at break (%)	T_{onset} (°C)	WVP (g mm/ m^2 h KPa)	Triple helix content (%)
25	2.1 ± 0,2[a]	51.5 ± 8,95[a]	3.31 ± 0.53[a]	266.5	0.16 ± 0.02[a]	13.5
35	1.0 ± 0,2[b]	20.9 ± 5,01[b]	3.57 ± 0.71[a]	252.6	0.23 ± 0.08[a]	8.7
80	1.2 ± 0,1[b]	19.1 ± 0,45[b]	2.98 ± 0.29[a]	251.4	0.24 ± 0.16[a]	0.3

Mean ± standard deviation. Mean values in the same column bearing the same letter are not statistically different according to the Tukey's test ($p > 0.05$).

Conclusion

Gelatin films reinforced with CNCs were successfully developed over a broad pH range. A comprehensive understanding of the pH role on the properties of Gel/CNCs films obtained by solution casting was provided by examining the possible electrostatic interactions and film structure involved. The different electric charges of gelatin chains attained at different pH led to different gelatin-gelatin and CNCs-gelatin interactions. Under electrostatic attractive forces (pH 3), the increase in the CNCs content resulted in the formation of complex coacervates. This behavior was not observed in the Gel/CNCs films above the Gel isoelectric point pH 6)I, The physical properties of gelatin films were significantly enhanced with the use of CNCs at 0.5 wt% CNCs and pH 8 due to the high triple helix content in the films. Furthermore, the drying temperature significantly hindered the gelatin triple helix formation, and consequently, had an inverse effect on the mechanical, thermal, and water barrier properties of the Gel/CNCs nanocomposites. In summary, modulating pH, CNCs amount, and drying temperature is a suitable strategy for tailoring the properties of nanocellulose-reinforced gelatin films to cover a broader range of requirements for food packaging applications. This strategy also illustrates a route for physicochemical control of the properties of polymer nanocomposites based on ionizable nanoparticles and polyelectryoles.

Credit Author Statement

Liliane Samara Ferreira Leite: Conceptualization, Methodology, Formal analysis, Investigation, Writing – original Draft. **Francys Kley Vieira Moreira:** Supervision, Conceptualization, Writing – review & Editing. **Luiz Henrique Capparelli Mattoso:** Supervision, Conceptualization, Writing – review & Editing. **Julien Bras:** Supervision, Conceptualization, Writing – review & Editing.

Declaration of competing interest

The authors declare that they have no known competing financial interests or personal relationships that could have appeared to influence the work reported in this paper.

Acknowledgments

This research was made possible thanks to the facilities of the Laboratory of Pulp and Paper Science and Graphic Arts (LGP2) that is part of the LabEx Tec 21 (Investissements d'Avenir - grant agreement n°ANR-11-LABX-0030) and of PolyNat Carnot Institute (Investissements d'Avenir - grant agreement n° ANR-16-CARN-0025-0), and Plant Macromolecule Research Center (CERMAV), which are acknowledged for the support to this work. This study was financed in part by CNPq, SISNANO (MCTI), FINEP, Embrapa AgroNano research network (Embrapa), Coordenação de Aperfeiçoamento de Pessoal de Nível Superior - Brazil (CAPES) [Finance Code 001] and by the São Paulo Research Foundation (FAPESP) [grant number 2016/03080-2 and 2018/00278-2]. We would like to thank Berthine Khelifi and Thierry Encinas from Grenoble Institute of Technology for their expertise in providing SEM imaging and XRD analyses, respectively.

Reference

Ahmed, J. (2017). Rheological properties of gelatin and advances in measurement. In *Advances in Food Rheology and Its Applications* (pp. 377–404). https://doi.org/10.1016/B978-0-08-100431-9.00015-2

Ahsan, S. M., & Rao, C. M. (2017). Structural studies on aqueous gelatin solutions: Implications in designing a thermo-responsive nanoparticulate formulation. *International Journal of Biological Macromolecules*, *95*, 1126–1134.

https://doi.org/10.1016/j.ijbiomac.20,,016.10.103
Al-Tayyar, N. A., Youssef, A. M., & Al-hindi, R. (2020). Antimicrobial food packaging based on sustainable bio-based materials for reducing foodborne pathogens: A review. *Food Chemistry*, *310*(December 2019), 125915. https://doi.org/10.1016/j.foodchem.2019.125915
Alberto, M., & Gabriela, M. (2012). Hydrodynamic Properties of Gelatin - Studies from Intrinsic Viscosity Measurements. *Products and Applications of Biopolymers*, (June). https://doi.org/10.5772/34401
Alexandre, E. M. C., Lourenço, R. V., Bittante, A. M. Q. B., Moraes, I. C. F., & Sobral, P. J. do A. (2016). Gelatin-based films reinforced with montmorillonite and activated with nanoemulsion of ginger essential oil for food packaging applications. *Food Packaging and Shelf Life*, *10*, 87–96. https://doi.org/10.1016/j.fpsl.2016.10.004
Alves, J. S., dos Reis, K. C., Menezes, E. G. T., Pereira, F. V., & Pereira, J. (2015). Effect of cellulose nanocrystals and gelatin in corn starch plasticized films. *Carbohydrate Polymers*, *115*, 215–222. https://doi.org/10.1016/j.carbpol.2014.08.057
Badii, F., MacNaughtan, W., Mitchell, J. R., & Farhat, I. A. (2014). The effect of drying temperature on physical properties oftThin gelatin films. *Drying Technology*, *32*(1), 30–38. https://doi.org/10.1080/07373937.2013.808206
Behrouzain, F., & Razavi, S. M. A. (2018). Steady shear rheological properties of emerging hydrocolloids. In *Emerging Natural Hydrocolloids* (pp. 81–100). https://doi.org/10.1002/9781119418511.ch1
Behrouzain, F., Razavi, S. M. A., & Joyner, H. (2020). Mechanisms of whey protein isolate interaction with basil seed gum: Influence of pH and protein-polysaccharide ratio. *Carbohydrate Polymers*, *232*(December 2019), 115775. https://doi.org/10.1016/j.carbpol.2019.115775
Bigi, A., Panzavolta, S., & Rubini, K. (2004). Relationship between triple-helix content and mechanical properties of gelatin films. *Biomaterials*, *25*(25), 5675–5680. https://doi.org/10.1016/j.biomaterials.2004.01.033
Cao, Y., Zavattieri, P., Youngblood, J., Moon, R., & Weiss, J. (2016). The relationship between cellulose nanocrystal dispersion and strength. *Construction and Building Materials*, *119*, 71–79. https://doi.org/10.1016/j.conbuildmat.2016.03.077
Celebi, H., & Kurt, A. (2015). Effects of processing on the properties of chitosan/cellulose nanocrystal films. *Carbohydrate Polymers*, *133*, 284–293. https://doi.org/10.1016/j.carbpol.2015.07.007
Chiou, B.-S., Avena-Bustillos, R. J., Bechtel, P. J., Jafri, H., Narayan, R., Imam, S. H., Orts, W. J. (2008). Cold water fish gelatin films: Effects of cross-linking on thermal, mechanical, barrier, and biodegradation properties. *European Polymer Journal*, *44*(11), 3748–3753. https://doi.org/10.1016/j.eurpolymj.2008.08.011
Chiou, B., Avena-bustillos, R. J., Bechtel, P. J., Imam, S. H., Glenn, G. M., & Orts, W. J. (2009). Effects of drying temperature on barrier and mechanical properties of cold-water fish gelatin films. *Journal of Food Engineering*, *95*(2), 327–331. https://doi.org/10.1016/j.jfoodeng.2009.05.011
da Silva, C. E. P., de Oliveira, M. A. S., Simas, F. F., & Riegel-Vidotti, I. C. (2020). Physical chemical study of zein and arabinogalactans or glucuronomannans polyelectrolyte complexes and their film-forming properties. *Food Hydrocolloids*, *100*(September 2019), 105394. https://doi.org/10.1016/j.foodhyd.2019.105394
Derkach, S. R., Kuchina, Y. A., Kolotova, D. S., & Voron'ko, N. G. (2020). Polyelectrolyte polysaccharide–gelatin complexes: Rheology and structure.

Polymers, *12*(2), 266. https://doi.org/10.3390/polym12020266
Derkach, S. R., Voron'ko, N. G., Sokolan, N. I., Kolotova, D. S., & Kuchina, Y. A. (2020). Interactions between gelatin and sodium alginate: UV and FTIR studies. *Journal of Dispersion Science and Technology*, *41*(5), 690–698. https://doi.org/10.1080/01932691.2019.1611437
Díaz-Calderón, P., Flores, E., Gonz, A., & Enrione, J. (2017). Influence of extraction variables on the structure and physical properties of salmon gelatin. *Food Hydrocolloids*, *71*, 118–128. https://doi.org/10.1016/j.foodhyd.2017.05.004
Díaz, O., Candia, D., & Cobos, Á. (2017). Whey protein film properties as affected by ultraviolet treatment under alkaline conditions. *International Dairy Journal*, *73*, 84–91. https://doi.org/10.1016/j.idairyj.2017.05.009
Dufresne, A. (2018). Cellulose nanomaterials as green nanoreinforcements for polymer nanocomposites. *Philosophical Transactions of the Royal Society A: Mathematical, Physical and Engineering Sciences*, *376*(2112), 20170040. https://doi.org/10.1098/rsta.2017.0040
Espino-Pérez, E., Domenek, S., Belgacem, N., Sillard, C., & Bras, J. (2014). Green process for chemical functionalization of nanocellulose with carboxylic acids. *Biomacromolecules*, *15*(12), 4551–4560. https://doi.org/10.1021/bm5013458
Esteghlal, S., Niakousari, M., & Hosseini, S. M. H. (2018). Physical and mechanical properties of gelatin-CMC composite films under the influence of electrostatic interactions. *International Journal of Biological Macromolecules*, *114*, 1–9. https://doi.org/10.1016/j.ijbiomac.2018.03.079
Fernando, M., Jorge, C., Humberto, C., Flaker, C., Fernandes, S., Cristina, I., … José, P. (2014). Viscoelastic and rheological properties of nanocomposite-forming solutions based on gelatin and montmorillonite. *Journal of Food Engineering*, *120*, 81–87. https://doi.org/10.1016/j.jfoodeng.2013.07.007
Gennadios, A., Brandenburg, A. H., Weller, C. L., & Testin, R. F. (1993). Effect of pH on properties of wheat gluten and soy protein isolate films. *Journal of Agricultural and Food Chemistry*, *41*(11), 1835–1839. https://doi.org/10.1021/jf00035a006
George, J., & Siddaramaiah. (2012). High performance edible nanocomposite films containing bacterial cellulose nanocrystals. *Carbohydrate Polymers*, *87*(3), 2031–2037. https://doi.org/10.1016/j.carbpol.2011.10.019
Gioffrè, M., Torricelli, P., Panzavolta, S., Rubini, K., & Bigi, A. (2012). Role of pH on stability and mechanical properties of gelatin films. *Journal of Bioactive and Compatible Polymers*, *27*(1), 67–77. https://doi.org/10.1177/0883911511431484
Gómez-Guillén, M. C., Pérez-Mateos, M., Gómez-Estaca, J., López-Caballero, E., Giménez, B., & Montero, P. (2009). Fish gelatin: a renewable material for developing active biodegradable films. *Trends in Food Science and Technology*, *20*(1), 3–16. https://doi.org/10.1016/j.tifs.2008.10.002
Habibi, Y., Lucia, L. A., & Rojas, O. J. (2010). Cellulose nanocrystals: chemistry, self-assembly, and applications. *Chemical Reviews*, *110*(6), 3479–3500. https://doi.org/10.1021/cr900339w
Hosseini, S. F., & Gómez-Guillén, M. C. (2018). A state-of-the-art review on the elaboration of fish gelatin as bioactive packaging: Special emphasis on nanotechnology-based approaches. *Trends in Food Science and Technology*, *79*(July), 125–135. https://doi.org/10.1016/j.tifs.2018.07.022
Hosseini, S. F., Rezaei, M., Zandi, M., & Farahmandghavi, F. (2015). Fabrication of bio-nanocomposite films based on fish gelatin reinforced with chitosan nanoparticles. *Food Hydrocolloids*, *44*, 172–182. https://doi.org/10.1016/j.foodhyd.2014.09.004

Joshi, N., Rawat, K., & Bohidar, H. B. (2018). pH and ionic strength induced complex coacervation of Pectin and Gelatin A. *Food Hydrocolloids*, *74*, 132–138. https://doi.org/10.1016/j.foodhyd.2017.08.011

Kwak, H. W., Lee, H., Park, S., Lee, M. E., & Jin, H.-J. (2020). Chemical and physical reinforcement of hydrophilic gelatin film with di-aldehyde nanocellulose. *International Journal of Biological Macromolecules*, *146*, 332–342. https://doi.org/10.1016/j.ijbiomac.2019.12.254

Leite, L. S. F., Ferreira, C. M., Corrêa, A. C., Moreira, F. K. V., & Mattoso, L. H. C. (2020). Scaled-up production of gelatin-cellulose nanocrystal bionanocomposite films by continuous casting. *Carbohydrate Polymers*, *238*(March), 116198. https://doi.org/10.1016/j.carbpol.2020.116198

Leite, Liliane S. F., Battirola, L. C., Escobar da Silva, L. C., & Gonçalves, M. do C. (2016). Morphological investigation of cellulose acetate/cellulose nanocrystal composites obtained by melt extrusion. ***J**. Appl. Polym. Sci.*, *44201*, 1–10. https://doi.org/10.1002/app.44201

Lin, L., Gu, Y., & Cui, H. (2019). Moringa oil/chitosan nanoparticles embedded gelatin nanofibers for food packaging against Listeria monocytogenes and Staphylococcus aureus on cheese. *Food Packaging and Shelf Life*, *19*(November 2018), 86–93. https://doi.org/10.1016/j.fpsl.2018.12.005

Li, Y., Zhang, X., Zhao, Y., Ding, J., & Lin, S. (2018). Investigation on complex coacervation between fish skin gelatin from cold-water fish and gum arabic: Phase behavior, thermodynamic, and structural properties. *Food Research International*, *107*(1), 596–604. https://doi.org/10.1016/j.foodres.2018.02.053

Lin, J., Pan, D., Sun, Y., Ou, C., Wang, Y., & Cao, J. (2019). The modification of gelatin films: Based on various cross-linking mechanism of glutaraldehyde at acidic and alkaline conditions. *Food Science and Nutrition*, *7*(12), 4140–4146. https://doi.org/10.1002/fsn3.1282

Mondragon, G., Peña-Rodriguez, C., González, A., Eceiza, A., & Arbelaiz, A. (2015). Bionanocomposites based on gelatin matrix and nanocellulose. *European Polymer Journal*, *62*, 1–9. https://doi.org/10.1016/j.eurpolymj.2014.11.003

Moustafa, H., Youssef, A. M., Darwish, N. A., & Abou-Kandil, A. I. (2019). Eco-friendly polymer composites for green packaging: Future vision and challenges. *Composites Part B: Engineering*, *172*(October 2018), 16–25. https://doi.org/10.1016/j.compositesb.2019.05.048

Noorbakhsh-Soltani, S. M., Zerafat, M. M., & Sabbaghi, S. (2018). A comparative study of gelatin and starch-based nano-composite films modified by nano-cellulose and chitosan for food packaging applications. *Carbohydrate Polymers*, *189*, 48–55. https://doi.org/10.1016/j.carbpol.2018.02.012

Qiao, C., Chen, G., Li, Y., & Li, T. (2013). Viscosity properties of gelatin in solutions of monovalent and divalent Salts. *Korea Australia Rheology Journal*, *25*(4), 227–231. https://doi.org/10.1007/s13367-013-0023-8

Qiao, C., Chen, G., Zhang, J., & Yao, J. (2016). Structure and rheological properties of cellulose nanocrystals suspension. *Food Hydrocolloids*, *55*, 19–25. https://doi.org/10.1016/j.foodhyd.2015.11.005

Quero, F., Padilla, C., Campos, V., Luengo, J., Caballero, L., Melo, F., … Enrione, J. (2018). Stress transfer and matrix-cohesive fracture mechanism in microfibrillated cellulose-gelatin nanocomposite films. *Carbohydrate Polymers*, *195*(January), 89–98. https://doi.org/10.1016/j.carbpol.2018.04.059

Razzak, M. A., Kim, M., & Chung, D. (2016). Elucidation of aqueous interactions between fish gelatin and sodium alginate. *Carbohydrate Polymers*, *148*, 181–188.

https://doi.org/10.1016/j.carbpol.2016.04.035
Santos, T. M., Souza Filho, M. D. S. M., Caceres, C. A., Rosa, M. F., Morais, J. P. S., Pinto, A. M. B., & Azeredo, H. M. C. (2014). Fish gelatin films as affected by cellulose whiskers and sonication. *Food Hydrocolloids*, *41*, 113–118. https://doi.org/10.1016/j.foodhyd.2014.04.001
Shiku, Y., Hamaguchi, P. Y., & Tanaka, M. (2003). Effect of pH on the preparation of edible films based on fish myofibrillar proteins. *Fishieries Science*, *69*, 1026–1032.
Silva, A. P. M., Oliveira, A. V., Pontes, S. M. A., Pereira, A. L. S., Souza Filho, M. de sá M., Rosa, M. F., & Azeredo, H. M. C. (2019). Mango kernel starch films as affected by starch nanocrystals and cellulose nanocrystals. *Carbohydrate Polymers*, *211*, 209–216. https://doi.org/10.1016/j.carbpol.2019.02.013
Voron'ko, N. G., Derkach, S. R., Kuchina, Y. A., & Sokolan, N. I. (2016). The chitosan-gelatin (bio)polyelectrolyte complexes formation in an acidic medium. *Carbohydrate Polymers*, *138*, 265–272. https://doi.org/10.1016/j.carbpol.2015.11.059
Vuillemin, M. E., Michaux, F., Muniglia, L., Linder, M., & Jasniewski, J. (2019). Gum Arabic and chitosan self-assembly: Thermodynamic and mechanism aspects. *Food Hydrocolloids*, *96*(May), 463–474. https://doi.org/10.1016/j.foodhyd.2019.05.048
Wang, Z., Zhou, J., Wang, X. xuan, Zhang, N., Sun, X. xiu, & Ma, Z. su. (2014). The effects of ultrasonic/microwave assisted treatment on the water vapor barrier properties of soybean protein isolate-based oleic acid/stearic acid blend edible films. *Food Hydrocolloids*, *35*, 51–58. https://doi.org/10.1016/j.foodhyd.2013.07.006
Yakimets, I., Wellner, N., Smith, A. C., Wilson, R. H., Farhat, I., & Mitchell, J. (2005). Mechanical properties with respect to water content of gelatin films in glassy state. *Polymer*, *46*(26), 12577–12585. https://doi.org/10.1016/j.polymer.2005.10.090
Yin, Y., Li, Z., Sun, Y., & Yao, K. (2005). A preliminary study on chitosan/gelatin polyelectrolyte complex. *Journal of Materials S*, *40*, 4646–4652. https://doi.org/10.1007/s10853-005-3929-9
Zhao, L., Skwarczynski, M., & Toth, I. (2019). Polyelectrolyte-based platforms for the delivery of peptides and proteins. *ACS Biomaterials Science & Engineering*, *5*(10), 4937–4950. https://doi.org/10.1021/acsbiomaterials.9b01135

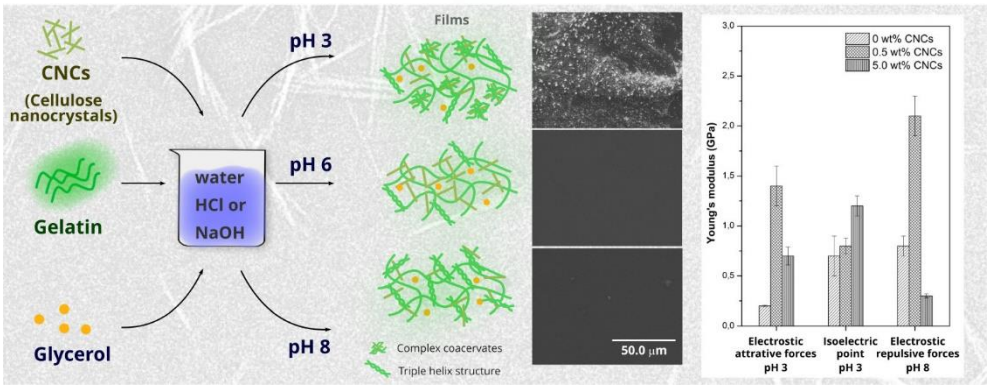
CNCs
(Cellulose nanocrystals)
Gelatin
Glycerol
water
HCl or
NaOH
pH 3
pH 6
pH 8
Films
Complex coacervates
Triple helix structure
50.0 µm
0 wt% CNCs
0.5 wt% CNCs
5.0 wt% CNCs
Young's modulus (GPa)
3,0
2,5
2,0
1,5
1,0
0,5
0,0
Electrostic attrative forces pH 3
Isoelectric point pH 3
Electrostic repulsive forces pH 8